Acta Cryst. (1975). A31, 161

Geometrical and Structural Relations in the Rhombohedral Perovskites

BY HELEN D. MEGAW
Cavendish Laboratory, Cambridge, England

AND C. N. W. DARLINGTON
Department of Physics, University of Birmingham, Birmingham, England

(*Received* 6 *June* 1974; *accepted* 23 *July* 1974)

The rhombohedral perovskites are of interest in lattice dynamics (*e.g.* $LaAlO_3$, $PrAlO_3$) and for their ferroelectric properties (*e.g.* $LiNbO_3$, $PbZr/TiO_3$). In this paper, data scattered through the literature are correlated, with correction of some misleading mistakes of calculation. Geometrical descriptions are put in a form allowing comparisons. The structures, classified by their space groups, are described in terms of four structural parameters, the octahedron tilt ω, octahedron distortion d, and A- and B-cation displacements s and t, together with an elongation or flattening ζ of the octahedron, deducible with the help of ω from the interaxial angle α_{rh}. Attention is drawn to the variety of physical causes underlying these departures from ideal perovskite. In the $R\bar{3}c$ structures a correlation not previously noted in the literature is found between the tilt angle ω and a flattening of the octahedron, and some tentative suggestions are made as to its cause. In the $R3m$ and $R3c$ structures, a lack of general correlation between B-cation displacement and the other parameters is noted, in contradiction to earlier reports.

1. Introduction

Rhombohedrally distorted perovskites have been attracting considerable attention in recent years in a number of different contexts. Some provide interesting studies in lattice dynamics (*e.g.* $LaAlO_3$ and $PrAlO_3$) or have unusual magnetic properties (*e.g.* $LaCoO_3$) or have interesting sequences of transitions (*e.g.* $KNbO_3$ and $NaNbO_3$); others are of technological as well as scientific importance for their ferroelectric properties [*e.g.* $Pb(Zr,Ti)O_3$ and $LiNbO_3$]. A number of new structures have been reported in the last ten years or so. These structures, although less symmetric than the aristotype (the ideal cubic structure), nevertheless have sufficiently high symmetry to allow discussion of structural details in terms of a very few parameters. It is the object of this paper to draw attention to relationships between the parameters, distinguishing between those of geometrical origin and those implying underlying physical causes, in the belief that, if the descriptive parameters of a 'static' structure are wisely chosen, they serve also as important parameters – often as the 'order parameters' – of its lattice dynamics.

We use the term 'perovskite' in a broad sense, to include not only $LiNbO_3$ and $LiTaO_3$ but also the transition-metal trifluorides, which have octahedral frameworks like other perovskites, but lack the cavity cation.

It has been shown (*e.g.* Megaw, 1968*b*; Moreau, Michel, Gerson & James, 1970) that rhombohedral perovskites can be described in terms of nearly regular BO_6 (or BF_6) octahedra, tilted (rotated) about the triad axis. The tilt angle ω is an important parameter of the structure. Moreover, independently of the tilting, some rhombohedral perovskites have displacements of A and B cations, from their polyhedron centres, along the triad axis.

We begin (§2) by considering the geometrical restrictions imposed by the trigonal symmetry, noticing some alternative ways of describing the facts. There are three different structures, distinguished by different space groups. Geometrical relations common to all are treated in §3. The relation between tilt angle ω and the interaxial angle α_{rh} of the rhombohedral unit cell put forward by Moreau *et al.* (1970), assuming regular octahedra, is re-derived in more general terms, and attention is called to the interesting deviation from their curve of the point for $LaAlO_3$ (mis-plotted by them) – a topic further developed, with additional evidence, in §5.

In §§4, 6, 7, 8 we consider the inter-relations between A-cation size, tilt angle, octahedron strain, and A and B-cation displacements. Though an empirical statement of these is a necessary first step, it is not in itself of much interest, unless it is used either to throw light on the physical interactions or to stimulate a search for explanation. From what follows, it is clear that a single 'explanation' will not suffice for compounds so varied as the rhombohedral perovskites, in spite of their similar geometry. We can however recognize some of the different factors involved, and examine their interactions. This is done in §4 and later sections. A general discussion follows in §10.

The analysis of perovskites in terms of octahedron deformation, octahedron tilt, and cation displacements, and the ideas put forward in these later sections, would, with suitable adaptation for the different geometry, be equally applicable to perovskites of other symmetries,

tetragonal and orthorhombic. Apart from a very brief comparison in §9, such a treatment is not attempted in the present paper.

2. Space groups, unit cells, and atomic position parameters

We make the assumption that, in rhombohedral perovskites, all BO_6 octahedra are related by space-group symmetry. This is empirically true not only for all known rhombohedral perovskites but also for most (though not all) perovskites of other symmetries; should exceptions later be discovered, ideas derived from structures satisfying the rule are likely to serve as a useful approach to them. The known rhombohedral perovskites are confined to space groups $R3m$, $R\bar{3}c$, or $R3c$, but in this section we shall consider all the rhombohedral space groups, from a geometrical standpoint.

It is convenient to describe all perovskite structures in terms of a pseudocubic unit cell whose axes correspond to those of the aristotype (ideal perovskite), with lattice parameters a_{pc}, $\alpha_{pc} \simeq 90°$. The possible structures fall into two categories. For those with space groups $R\bar{3}m$, $R3m$, $R32$, or $R3$, which are sub-groups of the aristotype space group $Pm3m$, the pseudocubic unit cell is nearly the same as that of the aristotype: it contains one formula unit, and has $a_{pc1} \simeq a_0 \simeq 4$ Å. For structures with space groups $R\bar{3}c$ or $R3c$, the pseudocubic unit cell has doubled edge lengths; it contains eight formula units, and has $a_{pc2} \simeq 2a_0 \simeq 8$ Å. This cell is all-face-centred. The only other rhombohedral space group, $R\bar{3}$, is excluded by the requirements of the perovskite linkage, which constrains the oxygen atoms into special positions satisfying the higher space group $R\bar{3}m$.

For the bipartite structures (space groups $R\bar{3}c$ and $R3c$), a more conventional, but less convenient, choice of unit cell corresponding to a primitive rhombohedral lattice contains two formula units and has $\alpha_{rh} \simeq 60°$. Comparison of interaxial angles in the two systems is easy, since, to a very good approximation,

$$90 - \alpha_{pc} = (\sqrt{3}/2)\,(60 - \alpha_{rh})\,. \qquad (1)$$

It is often convenient to use hexagonal axes of reference. Fig. 1(*a*) shows the orientations of the different sets of axes. The small ($a_{pc1} = a_0$) pseudocubic unit cell, for which the axes are not shown, gives rise to a hexagonal unit cell of the same base area as the large ($a_{pc2} = 2a_0$) but with half the height; it is however simpler to use the larger hexagonal cell throughout this paper. It should be noted that, while the primitive rhombohedron of the $R\bar{3}c$ and $R3c$ structures is in the conventional or *obverse* setting with respect to the hexagonal unit cell, the pseudocubic unit cell is in the unconventional or *reverse* setting. It seems less confusing to accept this than to use two different orientations of hexagonal axes, as would otherwise be necessary. Expressions for various transformations based on this figure are given in Table 1.

Each of the six space groups allows only one structure type with the perovskite topology. The atomic position parameters are listed in Table 2. These are not in the conventional form, but in a form which allows easy recognition of physically important features, with the same letter standing for displacements of corresponding direction and magnitude in the different space groups.

Consider first the array of oxygen atoms. In all six structures, this is a set of equally spaced planes normal to the triad axis. We have chosen the origin midway between such planes, not only for the space groups $R\bar{3}m$ and $R\bar{3}c$ where the point is a centre of symmetry,

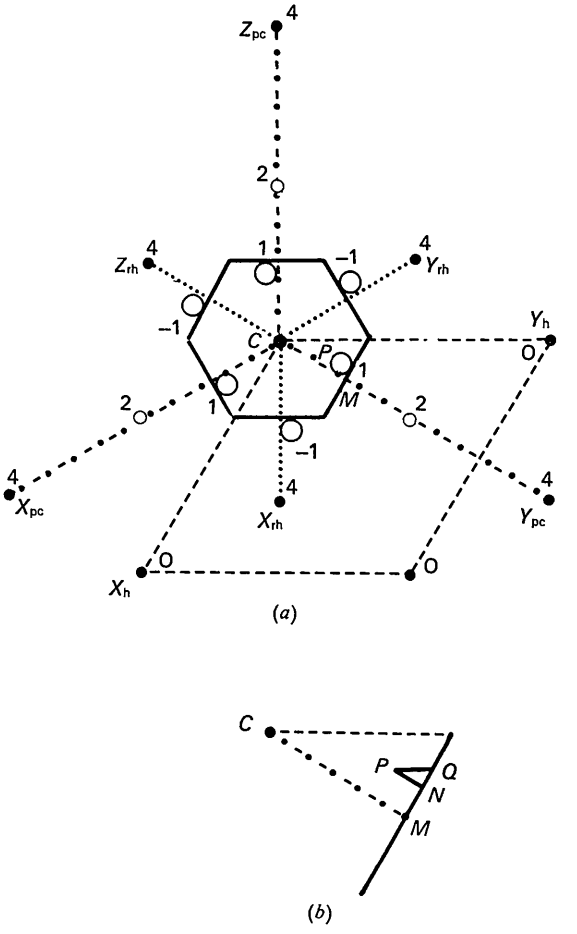

Fig. 1(*a*) Relationship between hexagonal (dashed), pseudocubic (dot–dash) and primitive rhombohedral (dotted) unit cells. Projection is down the triad axis; heights are in units of $c_H/12$. Small black circles are lattice points for $R\bar{3}c$ and $R3c$; small open circles are octahedron centres which would be lattice points for the pc1 cell. Large open circles are oxygen atoms, forming a slightly distorted octahedron about the B cation situated nearest the origin. *P* is the atom quoted in Table 2. The octahedron is rotated in an anti-clockwise direction about the triad axis and the parameter *d* is positive. (*b*) Enlargement of part of (*a*), showing possible positions of an oxygen atom. For $d = e = 0$, the oxygen is at *M*; for $d = 0$, $e > 0$, it is at *N*, and for $e > 0$, $d > 0$ it is at *P*. Thus $e = MN/2a_H$, $d = PN/4a_H$. cos 30°.

Table 1. *Matrices for translation between the different unit cells used for the rhombohedral perovskites*

The relation of the axes is shown in Fig. 1(*a*).

	Lattice parameters			Position parameters		
Large pseudocubic (pc2) in terms of primitive (~90°) rhombohedron of $R\bar{3}m$ and $R3m$ (pc1)	2	0	0	$\frac{1}{2}$	0	0
	0	2	0	0	$\frac{1}{2}$	0
	0	0	2	0	0	$\frac{1}{2}$
Large pseudocubic (pc2) in terms of primitive (~60°) rhombohedron of $R\bar{3}c$ and $R3c$ (rh)	1	$\bar{1}$	1	$\frac{1}{2}$	0	$\frac{1}{2}$
	1	1	$\bar{1}$	$\frac{1}{2}$	$\frac{1}{2}$	0
	$\bar{1}$	1	1	0	$\frac{1}{2}$	$\frac{1}{2}$
Hexagonal (H) in terms of large pseudocubic (pc2)	$\frac{1}{2}$	0	$\frac{\bar{1}}{2}$	$\frac{2}{3}$	$\frac{2}{3}$	$\frac{\bar{4}}{3}$
	$\frac{\bar{1}}{2}$	$\frac{1}{2}$	0	$\frac{\bar{2}}{3}$	$\frac{4}{3}$	$\frac{\bar{2}}{3}$
	1	1	1	$\frac{1}{3}$	$\frac{1}{3}$	$\frac{1}{3}$
Hexagonal (H) in terms of primitive (~60°) rhombohedron of $R\bar{3}c$ and $R3c$ (rh)	1	$\bar{1}$	0	$\frac{2}{3}$	$\frac{\bar{1}}{3}$	$\frac{\bar{1}}{3}$
	0	1	$\bar{1}$	$\frac{1}{3}$	$\frac{1}{3}$	$\frac{2}{3}$
	1	1	1	$\frac{1}{3}$	$\frac{1}{3}$	$\frac{1}{3}$

and for $R32$ where it is an intersection of axes, but also for $R3m$, $R3$, and $R3c$ which allow an arbitrary choice. Moreover, we quote the parameters for an oxygen atom on the *first* such plane above the origin, since this atom (at $z_H=\frac{1}{12}$ in the doubled cell) is a near neighbour to the B cation closest to the origin, whereas the conventionally quoted atom (at $z_H=\frac{1}{4}$) is more remote.

The meaning of the parameters d and e (or e') used in Table 2 is explained in Fig. 1(*b*). Displacements from the ideal position M are resolved into two components, MN perpendicular to CM, of length $2ea_H$, and PN parallel to CM, of length $(\sqrt{3}/2)PQ=(\sqrt{3}/2)4da_H$.

The parameter d describes a distortion* of the octahedron, keeping triad-axis symmetry, but making the sizes of the upper and lower faces different. This kind of distortion can only occur in the polar space groups $R3m$, $R3$, and $R3c$.

The parameters e' and e, which are independent of d, play different physical roles in the unipartite structures ($R32$ and $R3$) and the bipartite structures ($R\bar{3}c$ and $R3c$). In all cases, they indicate the rotation of an octahedron face about the triad axis; but in the unipartite structures the upper and lower faces rotate against each other, producing a distortion of shape of the octahedron, whereas in the bipartite structures they rotate in the same sense, producing a tilt (rotation) of the octahedron as a whole about the triad axis.

Since there are no perovskites yet known of the space groups $R32$ or $R3$, we shall not consider the parameter e' any further.

The parameter e is related to the tilt angle ω by the expression

$$\tan\omega=4\sqrt{3}e\,. \qquad (2)$$

We note that if $e=\frac{1}{12}$, corresponding to hexagonal close packing of oxygens, $\omega=30°$. (It is formally possible for ω to exceed 30°, and a description of calcite, $CaCO_3$, could be given in these terms. However, the physical differences are too great to make the formal isomorphism between calcite and the rhombohedral perovskites a matter of more than academic interest).

Another kind of deformation* of octahedron shape

* In this paper, we shall use the word 'deformation' for general departures from regularity of shape, keeping 'distortion' for the particular kinds of deformation described by the parameters d and e'.

Table 2. *Atomic position parameters for different choices of unit cell*

Space group	Atom	Type of unit cell: Primitive rhombohedron			Pseudocubic of side ≃ 8 Å			Hexagonal of height ≃ 14 Å		
$R\bar{3}m$	A	$\frac{1}{2}$	$\frac{1}{2}$	$\frac{1}{2}$	$\frac{1}{4}$	$\frac{1}{4}$	$\frac{1}{4}$	0	0	$\frac{1}{4}$
	B	0	0	0	0	0	0	0	0	0
	O	0	$\frac{1}{2}$	0	0	$\frac{1}{4}$	0	$\frac{1}{6}$	$\frac{1}{3}$	$\frac{1}{12}$
$R3m$	A	$\frac{1}{2}+2s$	$\frac{1}{2}+2s$	$\frac{1}{2}+2s$	$\frac{1}{4}+s$	$\frac{1}{4}+s$	$\frac{1}{4}+s$	0	0	$\frac{1}{4}+s$
	B	$2t$	$2t$	$2t$	t	t	t	0	0	t
	O	$2c'$	$\frac{1}{2}-4d$	$2d$	d	$\frac{1}{4}-2d$	d	$\frac{1}{6}-2d$	$\frac{1}{3}-4d$	$\frac{1}{12}$
$R32$	A	$\frac{1}{2}$	$\frac{1}{2}$	$\frac{1}{2}$	$\frac{1}{4}$	$\frac{1}{4}$	$\frac{1}{4}$	0	0	$\frac{1}{4}$
	B	0	0	0	0	0	0	0	0	0
	O	$-2e'$	$\frac{1}{2}$	$2e'$	$-e'$	$\frac{1}{4}$	e'	$\frac{1}{6}-2e'$	$\frac{1}{3}$	$\frac{1}{12}$
$R3$	A	$\frac{1}{2}+2s$	$\frac{1}{2}+2s$	$\frac{1}{2}+2s$	$\frac{1}{4}+s$	$\frac{1}{4}+s$	$\frac{1}{2}+s$	0	0	$\frac{1}{4}+s$
	B	$2t$	$2t$	$2t$	t	t	t	0	0	t
	O	$-2e'+2d$	$\frac{1}{2}-4d$	$2e'+2d$	$-e'+d$	$\frac{1}{4}-2d$	$e'+d$	$\frac{1}{6}-2e'-2d$	$\frac{1}{3}-4d$	$\frac{1}{12}$
$R\bar{3}c$	A	$\frac{1}{4}$	$\frac{1}{4}$	$\frac{1}{4}$	$\frac{1}{4}$	$\frac{1}{4}$	$\frac{1}{4}$	0	0	$\frac{1}{4}$
	B	0	0	0	0	0	0	0	0	0
	O	$\frac{1}{4}-2e$	$\frac{1}{4}+2e$	$-\frac{1}{4}$	$-e$	$\frac{1}{4}$	e	$\frac{1}{6}-2e$	$\frac{1}{3}$	$\frac{1}{12}$
$R3c$	A	$\frac{1}{4}+s$	$\frac{1}{4}+s$	$\frac{1}{4}+s$	$\frac{1}{4}+s$	$\frac{1}{4}+s$	$\frac{1}{4}+s$	0	0	$\frac{1}{4}+s$
	B	t	t	t	t	t	t	0	0	t
	O	$\frac{1}{4}-2e-2d$	$\frac{1}{4}+2e-2d$	$-\frac{1}{4}+4d$	$-e+d$	$\frac{1}{4}-2d$	$e+d$	$\frac{1}{6}-2e-2d$	$\frac{1}{3}-4d$	$\frac{1}{12}$

can occur besides those described by parameters d and e'. This is a homogeneous flattening or elongation along the triad axis, described by a factor $1+\zeta$, which can occur in all the space groups. We refer to it as *octahedron strain*. Unlike the distortions and the tilt angle, it cannot be derived from the atomic position parameters; instead, it can be deduced from the lattice parameters after allowance has been made for tilt. We shall consider this in §3.

The three parameters ζ, d, and e (or e') thus determine the shape and orientation of the BO_6 octahedron. Its size is expressed in terms of its average O–O edge length l.

We shall also be interested in cation displacements. Displacement of B from the octahedron centre is described by the position parameter t, that of A from an originally 12-coordinated site (at $z_H=\frac{1}{4}$) by the position parameter s. We shall use t' and s' to represent the corresponding displacements in Å. Such displacements can, of course, only occur in the polar space groups $R3m$, $R3$, or $R3c$. Geometrically s and t are independent; whether they are empirically related will be examined later, in §8.

The signs as well as the magnitudes of the position parameters s, t, d and e are of potential interest and need comment. Either s or t may be arbitrarily chosen as positive, because this merely determines the sense of c_H; whichever is given an arbitrary sign, the sign of the other must be found experimentally. The sign of e may be chosen arbitrarily; if we choose it as positive, it means that we take our origin at the centre of an octahedron whose tilt, viewed from above, is anticlockwise. On the other hand, the sign of d is not arbitrary, if a sign has already been allocated to s or t. If d is positive, as in Fig. 1(*a*), it means that the upper face of the octahedron is smaller, *i.e.* the face more distant from A if s is positive. The sign of d relative to that of s or t may thus carry interesting physical information.

3. Lattice parameters and tilt angle

We begin by considering the relation between tilt angle and lattice parameters. For the first step, we use hexagonal axes of reference.

Let the elongation or compression of the octahedron be defined by the factor $1+\zeta$, where ζ is the *octahedron strain*. Let l' be the length of the octahedron edges perpendicular to the triad axis (or the mean of such edges if the octahedron is distorted). Then

$$a_H = 2l' \cos\omega$$

$$c_{H2} = 6\sqrt{(2/3)}l'(1+\zeta)$$

whence

$$\frac{c_{H2}}{\sqrt{6}a_H} = \frac{1+\zeta}{\cos\omega}. \qquad (3)$$

The factor $\cos\omega$ obviously produces elongation of the hexagonal unit cell and hence of the pseudocubic unit cell along its triad axis; the factor $1+\zeta$ may act with this or against it, according to the sign of ζ. Using the identities

$$a_H^2 = \tfrac{1}{2}a_{pc}^2(1-\cos\alpha_{pc}) \qquad (4a)$$

$$c_H^2 = 3a_{pc}^2(1+2\cos\alpha_{pc}) \qquad (4b)$$

we have

$$\cos\alpha_{pc} = \frac{(1+\zeta)^2-\cos^2\omega}{(1+\zeta)^2+2\cos^2\omega}. \qquad (5)$$

Since ζ is always small (of the order of $\sin^2\omega$) this may be written

$$\cos\alpha_{pc} = \frac{\sin^2\omega}{3-2\sin^2\omega} + \frac{(2/3)\zeta}{1-(2/3)\sin^2\omega}. \qquad (6)$$

The first term in (6) represents the calculated value of α_{pc} assuming regular octahedra ($\zeta=0$). It is always positive. Thus, for regular octahedra, α_{pc} is always less than 90°, and α_{rh} less than 60°, from (1). To demonstrate this for α_{rh} directly, we rewrite the expression of Moreau *et al.* (1970) (their equation 3) as

$$\cos\alpha_{rh} = \frac{4-\cos^2\omega}{4+2\cos^2\omega} = \frac{1}{2} + \frac{\sin^2\omega}{3-\sin^2\omega} \gg \frac{1}{2}. \qquad (7)$$

If the observed value of α_{pc} differs from that calculated assuming regularity, and experimental error can be neglected, we have

$$\cos(\alpha_{pc})_{obs} - \cos(\alpha_{pc})_{calc} = (\tfrac{2}{3})\zeta[1-(\tfrac{2}{3})\sin^2\omega]^{-1}. \qquad (8)$$

The octahedron strain ζ can thus easily be deduced from a comparison of calculated and observed interaxial angles, provided that sufficiently accurate data are available.

In Fig. 2, ω is plotted against $90-\alpha_{pc}$ for all the materials for which experimental information is available. The data concerning the oxide perovskites are

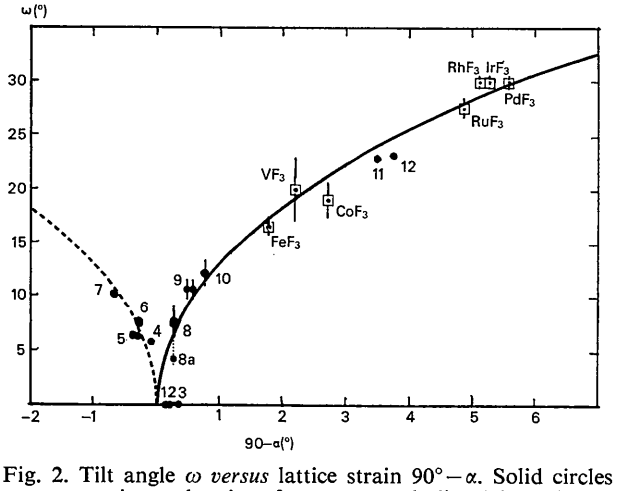

Fig. 2. Tilt angle ω *versus* lattice strain $90°-\alpha$. Solid circles are experimental points for compounds listed in Table 3, and open squares those for trifluorides. Error bars in ω are derived from information in the original papers; for points 4,5,6,7,11,12 they are of the order of 0·1°, too small to show here. The full line is the theoretical curve assuming regular octahedra, the dashed line an empirical guide line constructed by reflecting the full line at $90°-\alpha$.

given, with references, in Table 3; those for the trifluorides are taken directly from the work of Hepworth, Jack, Peacock & Westland (1957). The smooth curve is that calculated for regular octahedra, for which $(\cos \alpha_{pc})_{calc}$ is given by the first term in equation (6).

The part of the figure corresponding to positive values of $90° - \alpha_{pc}$ resembles that of Moreau *et al.* (1970) except that $90° - \alpha_{pc}$ has been used instead of $60° - \alpha_{rh}$, and some new points have been inserted. There is, however, a vital difference concerning $LaAlO_3$. The experimental value of α_{pc} is *greater* than 90°, and of α_{rh} *greater* than 60° (Geller & Bala, 1956). The point cannot possibly lie on their theoretical curve.*

New work shows that all other nearly cubic perovskites of space group $R\bar{3}c$ also have negative values of $90 - \alpha_{pc}$, implying flattened octahedra. The observed points lie near an empirical curve drawn for

$$(\cos \alpha_{pc})_{emp} = -(\cos \alpha_{pc})_{calc} . \qquad (9)$$

* Michel, Moreau & James (1971), who put forward a very similar diagram, also give a table of lattice parameters for the points plotted, but without reference to their experimental source. Both for $LaAlO_3$ and for $LaCoO_3$ (Wold, Post & Banks, 1957) the values tabulated by Michel *et al.* (1971) appear to be *calculated* values derived from the observed ω assuming the regular octahedra they are trying to prove. In a later note, Michel, Moreau & James (1972) give a correction of lattice parameters of $LaAlO_3$, but do not mention the significance of the corresponding change in a_{rh}.

These materials will be considered further in §5.

The other deviations from the calculated curve are smaller. All points for structures of space group $R3m$ lie to the right of the curve, indicating elongated octahedra. Of the oxides of space group $R3c$, only the compounds of the smallest cation, Li, lie significantly to the right. The other three lie close to the curve; the data are not very precise, and any deviations from regularity of the octahedron are probably within experimental error. The trifluorides also lie close to the curve, except for RhF_3 and IrF_3, for which the octahedra are significantly flattened, as noted by Hepworth *et al.* (1957) – who also commented that the specimen of CoF_3 gave somewhat diffuse reflexions.

The octahedron strains in the oxides have been calculated using equation (8) and are recorded in Table 3. Discussion follows in §5 and §6. The trifluorides will not be considered further.

4. Tilt angle and A-cation size

The use of any set of empirical radii requires caution. Such sets are based implicitly on the assumption that atoms can be treated as rigid spheres of constant radius; in so far as this is not true, corrections and adaptations will be needed. In constructing any such tables, averaging and interpolation procedures have been used, which are inevitably to some extent subjective,

Table 3. *Rhombohedral angle, tilt angle, and octahedron strain*

	Space group	Compound*	α_{pc}	ω°	$\cos \alpha_{pc} \times 10^2$ calc	$\cos \alpha_{pc} \times 10^2$ obs	Octahedron strain $\zeta \times 10^2$	Reference α	Reference ω
1	$R3m$	$BaTiO_3$(−90 °C)	89°52′	0	0	0·23	0·35	8	
2	$R3m$	$KNbO_3$(−43 °C)	89°49′	0	0	0·32	0·48	6	
3	$R3m$	$Pb(Zr_{0.58}Ti_{0.42})O_3$	89°39′	0	0	0·61	0·92	11	
4	$R\bar{3}c$	$LaAlO_3$	90°05′	5·8	0·34	−0·15	−0·73	5	12
5	$R\bar{3}c$	$PrAlO_3$†	90°17′ / 90°21′	6·5	0·43	−0·50 / −0·61	−1·37 / −1·55	5 / 3	3
6	$R\bar{3}c$	$BaTbO_3$	90°17′	7·5	0·57	−0·50	−1·59	7	7
7	$R\bar{3}c$	$LaCoO_3$	90°42′	10·3	1·09	−1·22	−3·39	15	9
8	$R3c$	$Pb(Zr_{0.90}Ti_{0.10})O_3$	89°44′	7·5	0·57	0·47	(−0·15)‡	11	11
8*a*	$R3c$			4·3	0·19		0·42		16
9	$R3c$	$BiFeO_3$†	89°24′ / 89°31′	10·6	1·15	1·05 / 0·84	(−0·15)‡ / (−0·45)‡	14 / 13	10
10	$R3c$	$NaNbO_3$(*N*) (−150 °C)	89°13′	12·1	1·51	1·37	(−0·21)‡	4	4
11	$R3c$	$LiTaO_3$	86°32′	22·9	5·61	6·05	0·59	1	1
12	$R3c$	$LiNbO_3$	86°16′	23·1	5·72	6·51	1·08	2	2

* All at room temperature except where other temperatures are noted.
† Different values of α obtained by different workers.
‡ Strains probably within limits of experimental error.

Key to references

1. Abrahams & Bernstein (1967). Abrahams, Hamilton & Sequiera (1967). 2. Abrahams, Reddy & Bernstein (1966). Abrahams, Hamilton & Reddy (1966). 3. Burbank (1970); there is an arithmetical inconsistency in the paper, and Dr Burbank has confirmed (personal communication) that the correct value of should be 6·5°. 4. Darlington & Megaw (1973). 5. Geller & Bala (1956). 6. Hewat (1973). 7. Jacobson, Tofield & Fender (1972); their conclusion that the octahedron is regular is inconsistent with their measurements; regularity would give α_{rh} as 59°37′, as compared with the observed 60°25′. 8. Kay & Vousden (1949). 9. Menyak, Dwight & Raccah (1967). 10. Michel, Moreau, Achenbach, Gerson & James (1969*a*). 11. Michel, Moreau, Achenbach, Gerson & James (1969*b*). 12. Müller, Berlinger & Waldner (1968). 13. Tomašpol'skij, Venevcev & Ždanov (1964). 14. Venevcev, Ždanov, Solov'ev, Bezus, Ivanova, Fedulov & Kapyšev (1960). 15. Wold, Post & Banks (1957). 16. A. M. Glazer, preliminary results of a new studv (personal communication).

and biased towards those materials on which the fullest experimental work has been done. It follows that, though the radii are of great value for a general understanding of structures, and in more detail for making comparisons between isomorphous materials, we have to be on our guard against attaching too much importance to small discrepancies in absolute values.

Radii used in the present work are those of Shannon & Prewitt (1969, 1970), except that, where radii for nine-coordination are not given, or are doubtful, they have been found by interpolation. For the oxygen radius, r_O, the value of 1·40 Å has been taken, somewhat arbitrarily; since we use it only to study the variation of the radius sum, r_A+r_O, the absolute value is not of importance.

Fig. 3 shows the geometrical effects of tilting, and Table 4 gives some of the interatomic distances and bond angles in terms of structural parameters.

Packing principles suggest that the short A–O distance *CF* is equal to the sum of the radii, r_A+r_O. Neglecting for present purposes the effects of cation displacements s and t (which are small if not zero), and the possible distortion d, we can allow for the differences of size of different B octahedra by taking the ratio $(r_A+r_O)/l$, where l is the observed octahedron edge length. This ratio corresponds to the Goldschmidt tolerance factor. We expect a smooth variation of ω with this quantity.

The radii and the values of $(r_A+r_O)/l$ are given in Table 5, both for six-coordination and for the observed coordination numbers in the different materials. In Fig. 4 $(r_A+r_O)/l$ is plotted against ω.

With points calculated for six-coordinated radii, the expected smooth curve can be drawn passing reasonably close to all but three of them. With those assuming the observed coordination number, the same is true provided we ignore the two points for compounds with the smallest A-cation, Li. The other exceptions are the same in both cases: for $PbZr_{0.58}Ti_{0.42}O_3$ ω is anomalously small, and also for $PbZr_{0.90}Ti_{0.10}O_3$, according to the most recent work (M. Glazer, personal communication), while for $LaCoO_3$ it is anomalously large. Anomalous behaviour is to be expected in the two former, because of the tendency of Pb to form anisotropic

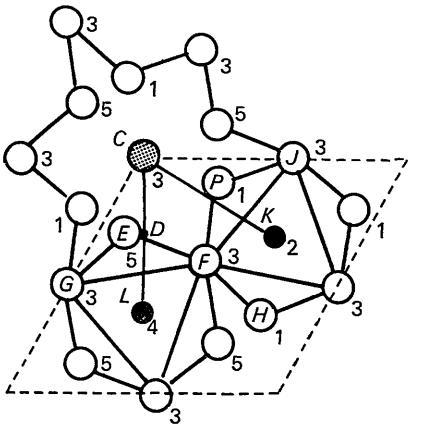

Fig. 3. Geometry of structure with tilt, projected down triad axis. Base of hexagonal cell is outlined by the dashed lines; lines *CL* and *CK* are at right angles to them. Figures give heights of atoms in units of $c_H/12$; only those between heights 1 and 5 inclusive are shown. Hatched circle, A cation; solid circles, B cations; open circles, oxygen. Full lines are edge of octahedron (those in planes at heights 1 and 5 being omitted). For comparison with the text and Table 4, letters refer to atoms at the heights indicated; the same letters with dashes refer to their projection in the plane of the diagram. The tilt angle ω is $D'C'E'=D'L'E'$.

Table 4. *Bond lengths and angles*

Bond lengths as multiples of $a_H/(2\cos\omega)$

Bond type	Reference to Fig. 3	General expression	Approximation*
A–O	*CF*	$[1-(\sqrt{3}/3)\sin 2\omega-(2/3)\sin^2\omega+6s^2(1+\zeta)^2+48d^2\cos^2\omega]^{1/2}$	$[1-(\sqrt{3}/3)\sin 2\omega-(2/3)\sin^2\omega+6s^2]^{1/2}$
	CG	$[1+(\sqrt{3}/3)\sin 2\omega-(2/3)\sin^2\omega+6s^2(1+\zeta)^2+48d^2\cos^2\omega]^{1/2}$	$[1+(\sqrt{3}/3)\sin 2\omega-(2/3)\sin^2\omega+6s^2]^{1/2}$
	CP	$[1+(2/3)\{(1+6s)^2(1-\zeta)^2-1\}-8d\cos^2\omega+48d^2\cos^2\omega]^{1/2}$	$[1+8s+24s^2+(4/3)\zeta]^{1/2}$
	CE	$[1+(2/3)\{(1-6s)^2(1+\zeta)^2-1\}+8d\cos^2\omega+48d^2\cos^2\omega]^{1/2}$	$[1-8s+24s^2+(4/3)\zeta]^{1/2}$
B–O	*LE*	$(\sqrt{2}/2)[1+(1/3)\{(1-12t)^2(1+\zeta)^2-1\}-16d\cos^2\omega+96d^2\cos^2\omega]^{1/2}$	$(\sqrt{2}/2)[1-8t+48t^2+(2/3)\zeta]^{1/2}$
	LF	$(\sqrt{2}/2)[1+(1/3)\{(1+12t)^2(1+\zeta)^2-1\}+16d\cos^2\omega+96d^2\cos^2\omega]^{1/2}$	$(\sqrt{2}/2)[1+8t+48t^2+(2/3)\zeta]^{1/2}$
O–O	*FJ*	$[1-24d\cos^2\omega+144d^2\cos^2\omega]^{1/2}$	1
	FG	$[1+24d\cos^2\omega+144d^2\cos^2\omega]^{1/2}$	
	FE	$[1+(2/3)\{(1+\zeta)^2-1\}+4\sqrt{3}d\sin 2\omega+144d^2\cos^2\omega]^{1/2}$	$[1+(4/3)\zeta]^{1/2}$
	GE	$[1+(2/3)\{(1+\zeta)^2-1\}-4\sqrt{3}d\sin 2\omega+144d^2\cos^2\omega]^{1/2}$	

Angle	Approximation*
O–B–O	$\cos FLG=(2/3)\zeta+8t-16t^2$
	$\cos FKJ=(2/3)\zeta-8t-16t^2$
	$\cos FLE=-(2/3)\zeta+48t^2$
B–O–B	$\cos KFL=1-(4/3)\sin^2(\frac{1}{2}\omega)-64t^2$

* The approximation neglects all terms in d, and all but first-order tems in ζ and second-order terms in s and t.

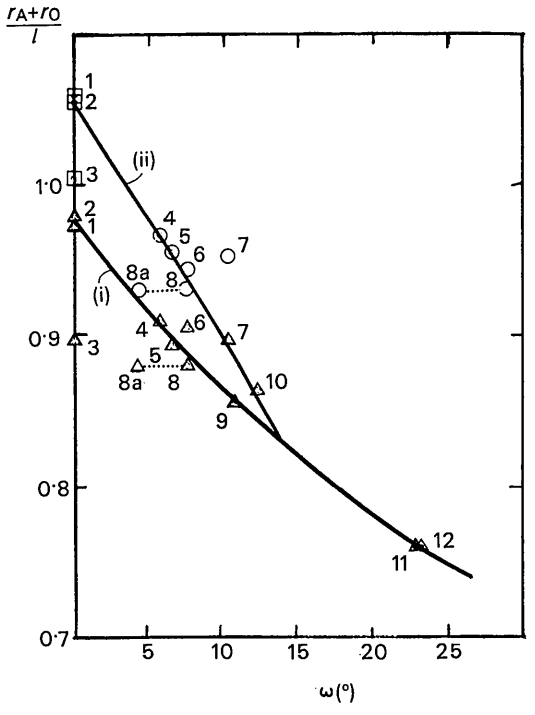

Fig. 4. Ratio $(r_A+r_O)/l$ *versus* ω. Points marked by squares, circles, and triangles use r_A values for coordination numbers 12,9 and 6 respectively; key numbers refer to Table 5. Curve (i) is drawn empirically through points for six-coordination, curve (ii) through those for the actual coordination number of the structure (excluding points 11 and 12).

directed bonds;* the last-named will need further consideration in §5.

The part of the curve drawn for nine-coordination can be used, by interpolation, to predict ω values for other perovskites known to be isomorphous with $LaAlO_3$ whose position parameters have not been measured experimentally. These are given in Table 5. A value for $SmAlO_3$ has been included, but must be regarded as a hypothetical extrapolation, because the rhombohedral structure in this material is only found above a transition at 850°C, while predictions based on empirical radii refer to room temperature.

5. Tilt angle and octahedron strain in $R\bar{3}c$ structure

The four points at the left of Fig. 2 suggest, empirically, that a correlation exists between negative octahedron strain and tilt angle. To test this further, we use evidence provided by high-temperature measurements on $LaAlO_3$ (Geller & Bala, 1956; Müller, Berlinger & Waldner, 1968), and by the isomorphous compounds for which ω was estimated in §4 and for which room-temperature experimental measurements of α_{pc} have been made. Where different workers give different values for α_{pc}, calculations are here made for both, to indicate the possible limits of error. The observed val-

* It is worth noting that $PbZr_{0.58}Ti_{0.42}O_3$ is the only compound, of all those considered, in which the distortion d has been reported to be significantly large – *cf.* §6.

Table 5. *Tilt angle and A-cation size*

Key No.	Compound	C.N.	r_A (Å)	r_A+r_O (Å)	Obs. l (Å)	Ratio $(r_A+r_O)/l$	ω obs	ω est
1	$BaTiO_3$	12	1·60	3·00	2·836	1·058	0	
		6	1·36	2·76		0·973		
2	$KNbO_3$	12	1·60	3·00	2·839	1·056	0	
		6	1·38	2·78		0·979		
3	$Pb(Zr_{0.58}Ti_{0.42})O_3$	12	1·49	2·89	2·877	1·004	0	
		6	1·18	2·58		0·897		
4	$LaAlO_3$	9	1·20	2·60	2·69	0·966	5·8°	
		6	1·05	2·45		0·909		
5	$PrAlO_3$	9	1·17	2·57	2·69	0·955	6·5°	
		6	1·00	2·40		0·982		
6	$BaTbO_3$	9	1·47	2·87	3·044	0·943	7·5°	
		6	1·36	2·76		0·906		
7	$LaCoO_3$	9	1·20	2·60	2·73	0·952	10·3°	
		6	1·05	2·45		0·897		
8	$Pb(Zr_{0.90}Ti_{0.10})O_3$	9	1·33	2·73	2·93	0·932	7·5°	
		6	1·18	2·58		0·880		
9	$BiFeO_3$	6	1·02	2·42	2·83	0·855	10·6°	
10	$NaNbO_3(N)$	6	1·02	2·42	2·804	0·863	12·1°	
11	$LiTaO_3$	6	0·74	2·14	2·810	0·760	22·9°	
12	$LiNbO_3$	6	0·74	2·14	2·810	0·760	23·1°	
13	$CeAlO_3$	9	1·18	2·58	2·69*	0·958		6·2±0·4°
14	$NdAlO_3$	9	1·16	2·56	2·69*	0·951		6·8±0·4°
15	$SmAlO_3$	9	1·13	2·53	2·69*	0·941		7·4±0·4°
16	$LaGaO_3$	9	1·20	2·60	2·80†	0·928		7·8±0·4°

* Taken equal to that in $LaAlO_3$.
† Calculated from r_B+r_O.

ues of α and calculated values of ζ are recorded in Table 6, and in Fig. 5 ζ is plotted against ω.

It is obvious from this graph that there is a consistent trend. Even $LaCoO_3$, with its anomalously large ω, fits in smoothly with the rest. Since there is no geometrical connexion between ζ and ω, this implies some physical relationship. *The tilt angle and the octahedron strain are coupled in some way by the structure.*

It is not possible to give a simple explanation of the origin of this coupling. In Fig. 5, curves (i) and (ii), which fit the observed points moderately well, are purely empirical. Curve (i) corresponds to the dashed curve in Fig. 2, for which, from equations (9) and (6)

$$-\zeta=\sin^2\omega\,. \qquad (10)$$

Curve (ii) is given by

$$-\zeta=\tfrac{1}{2}\omega^2+3\omega^3. \qquad (11)$$

The latter is a good fit for all the compounds of La, and also for $BaTbO_3$, but the aluminates of the smaller A-cations all lie above it.

We can, however, show that packing principles are inadequate to explain the facts, and we can make some tentative suggestions as to where an explanation may be found.

The argument from packing runs as follows. Tilting decreases one set of A–O distances (*CF* in Fig. 3) until they equal r_A+r_O. The other set (such as *CE*) are little altered. The inequality can be reduced by compressing the octahedron, but at the cost of introducing new inequalities between the O–O distances. If we suppose that both kinds of inequality are energetically unfavourable, we may reasonably expect a balance between them, making ζ dependent not only on ω but on the relative 'deformabilities' of the A and B polyhedra. We should then predict, for a given ω, that ζ will be small when B is small and its octahedron therefore less easily deformed.

Unfortunately this not borne out by the facts. Though B is smallest for the aluminates, the points for these (except $LaAlO_3$) lie rather *above* the curve through the rest.

Moreover, a worse difficulty is found in $LaCoO_3$. As we saw in §4, ω is anomalously large; it corresponds to a length 2·43 Å for La–O, as compared with 2·52 Å in $LaAlO_3$. We might try to modify the argument, recognizing that the forces in the CoO_6 octahedron are not simply ionic, and that flattening may be due to a Jahn–Teller effect. In support of this it may be noted that $LaCoO_3$ has interesting magnetic properties (Menyuk, Dwight & Raccah, 1967). Though plausible in itself, this assumption fails to explain the coupling: the argument provides no reason why shortening of the longer A–O bonds should also shorten those that are already short.

In so far as cation–cation repulsions play a role, it might be argued that flattening of the octahedra serves to counteract the inequalities of cation–cation distance

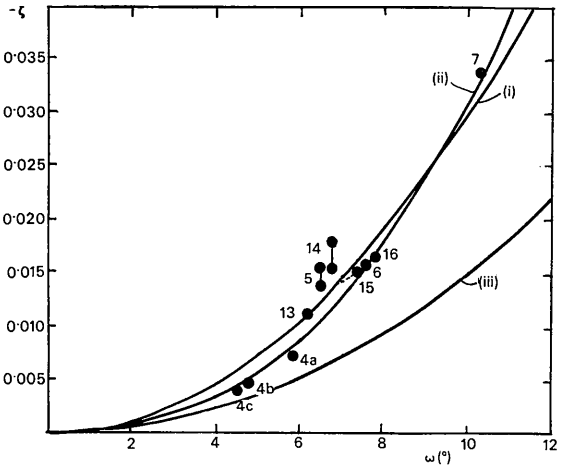

Fig. 5. Octahedron strain ξ *versus* tilt angle ω. Key numbers of points as in Table 6. Dotted line to left of point 15 ($SmAlO_3$) indicated nature of correction to allow for the fact that the true value of ω at 850° must be less than the estimated R.T. value. Curve (i): $-\xi=\sin^2\omega$ (empirical). Curve (ii): $-\xi=\frac{1}{2}\omega^2+3\omega^3$ (empirical). Curve (iii): $-\xi=2\sin^2\omega/2$ (condition for equal cation–cation distances).

Table 6. *Tilt angle and octahedron strain in $R\bar{3}c$ structures*

Key No.	Compound	Temperature	α–90°	ω(°) obs.	ω(°) est.	Octahedron Strain ζ
4*a*	$LaAlO_3$	R.T.	5′	5·8		−0·0073
4*b*	$LaAlO_3$	200°C	3′	4·8		−0·0048
4*c*	$LaAlO_3$	250°C	2′	4·5		−0·0039
5	$PrAlO_3$	R.T.	17′ / 21′ *	6·5		−0·0137 / −0·0155
6	$BaTbo_3$	R.T.	17′	7·5		−0·0159
7	$LaCoO_3$	R.T.	42′	10·3		−0·0339
13	$CeAlO_3$	R.T.	13′	6·2 (4)†		−0·0115 (9)†
14	$NdAlO_3$	R.T.	25′ / 19′ *	6·8 (4)†		−0·0179 (9)† / −0·0152 (9)†
15	$SmAlO_3$	850°C	16′	7·4 (4)†		−0·0152 (9)†
16	$LaGaO_3$	R.T.	17′	7·8 (4)†		−0·0165 (9)†

* Different experimental values measured by different workers.
† Estimated errors arising from interpolation.

produced by the tilt. This would be true if ζ were limited by the relation making the structure metrically cubic, *i.e.*

$$1+\zeta \geq \cos \omega ,$$

whence

$$-\zeta \leq 2 \sin^2 \omega/2 \sim \tfrac{1}{2}\omega^2. \qquad (12)$$

This has been plotted as curve (iii) in Fig. 5. It can be seen that the observed value of $|\zeta|$ is always greater than the hypothetical limit; indeed, it is such as to *create* large inequalities of the opposite sign from those associated with regular octahedra. This effect therefore fails to explain the coupling.

We have thus to go beyond simple packing and electrostatic ideas and consider the role of semipolar bonding. The similarity of the coupling for very different A and B cations directs our attention to the oxygen atom which is common to the whole series.

Our basic assumption is that changes in the anisotropic electron distribution round O due to one kind of neighbour can affect the 'contact distances' for other kinds of neighbours, *i.e.* the distances at which the repulsive forces become effectively infinite. The tendency to form B–O–B angles of less than 180°, when contact distances allow it, is here assumed to be the cause of the tilt; the deviation from 180° is nearly proportional to ω (*cf.* Table 4, last line). If the consequent redistribution of orbitals shortens the effective radius towards the oxygen neighbours in layers above and below, but not towards those in the same horizontal plane, flattening of the octahedron follows. Conversely, if the flattening is due to an intrinsic cause, as in $LaCoO_3$, shortening of the sloping O–O edges gives rise, by the same coupling mechanism, to an increase in B–O–B bond angle, which causes an abnormal shortening of the short La–O bond.

Though packing principles have proved inadequate to explain the octahedron strain in these compounds, it must be remembered that the effect is geometrically a second-order one, with $\zeta \sim \omega^2$. The above treatment, while not quantitative, may indicate how a bond-theory approach would be related to the older, simpler, use of rigid ions, which can still serve us well as a first approximation.

6. Octahedron distortion, octahedron strain, and B-cation displacement in *R*3*m* and *R*3*c* structures

Table 7 lists the distortion parameter d and the cation displacement parameters s and t.

The distortion parameter is generally very much smaller than the other parameters; except for $Pb(Zr_{0.58}Ti_{0.42})O_3$ it can be neglected for the purposes of this paper. Its significance in $LiNbO_3$ has been discussed elsewhere (Darlington & Megaw, 1973) and the same considerations apply to the isomorphous $LiTaO_3$. For $Pb(Zr_{0.58}Ti_{0.42})O_3$, it is so large that approximations neglecting it become unsafe, but it remains unexplained, though almost certainly associated with the formation of directed bonds. We note that in all cases the sign is negative, except in $KNbO_3$, where the magnitude is not much greater than experimental error.

The B-cation displacement, in these polar space groups, gives rise to a dipole and hence to a spontaneous polarization. Abrahams, Kurtz & Jamieson (1968) have suggested that P_s is proportional to the displacement, with a roughly universal constant of proportionality for different materials. It is therefore tempting to explain the 'spontaneous strain' as the consequence of the spontaneous polarization, by analogy with the familiar macroscopic relation between induced strain and induced polarization in a homogeneous material

$$\text{strain} \propto P_s^2 , \qquad (13)$$

identifying 'spontaneous strain' with octahedron strain ζ. We must of course distinguish between the assumption of the relation for a single material under different conditions of temperature and pressure, and its extension to what concerns us here, a range of very different materials. In the former case, it is plausible to assume one constant of proportionality, characteristic of the material, but there is no reason at all to expect the

Table 7. *Octahedron distortion, cation position parameters, and cation displacements in R*3*m and R*3*c structures*

Key No.	Compound	Position parameters* d	s	t	Displacements† s' (Å)	t' (Å)	$(t')^2$ $\times 10^2$	ζ $\times 10^2$	ω (°)
2	$KNbO_3$(−43 °C)	~0·002	0·009	0·0156	0·13 (3)	0·22 (1)	4·7	0·48	0
3	$PbZr_{0.58}Ti_{0.42}O_3$	−0·019	0·017	0·010	0·23 (?)	0·13 (?)	1·7	0·92	0
8	$PbZr_{0.90}Ti_{0.10}O_3$	0	0·022	0·007	0·32 (2)	0·10 (2)	1·0	−0·15	7·5
8*a*		−0·003	0·027	0·006	0·39	0·09	0·8	0·42	4·3
9	$BiFeO_3$‡	−0·004	0·045	0·017	0·62 (3)	0·23 (3)	5·3	−0·15 / −0·45	10·6
10	$NaNbO_3$(*N*) (−150 °C)	0	0·022	0·016	0·31 (0)	0·23 (1)	5·3	−0·21	12·1
11	$LiTaO_3$	−0·0026	0·044	0·014	0·60 (2)	0·20 (1)	4·0	0·59	22·9
12	$LiNbO_3$	−0·0028	0·051	0·019	0·71 (2)	0·27 (1)	6·6	1·08	23·1

* Defined as in Table 2.
† Figures in brackets are estimated errors, in units of the last digit quoted.
‡ A recent refinement by Jacobson & Fender (private communication) gives parameters differing only slightly from these.

constant to be a universal one, the same – or nearly so – for all materials. We nevertheless test the assumption; Table 1 gives values of t', the B-cation displacement, and of $(t')^2$ and ζ. It can be seen that there is no consistent relationship. We note in particular the small, possibly negative, values of the strain for $NaNbO_3$ and $BiFeO_3$, whose t' values are intermediate between those of $LiTaO_3$ and $LiNbO_3$, both with large positive strains.

It might be argued that, in $R3c$ structures, the observed strain is the sum of an elongation due to the spontaneous polarization and a flattening like that in the $R\bar{3}c$ structure (§5). This is not impossible, but three considerations make any conclusion unsafe: the lack of a quantitative theory of the flattening effect, the uncertainty of extrapolation of an ill-defined empirical curve, and the considerable differences likely to result from non-zero values of the A displacement.

The treatment by Megaw (1968*c*) of the relations between octahedron strain and B-cation displacements of different symmetries would suggest that, for rhombohedral perovskites, there should be no strain directly due to B displacement. Indirect effects, linking B displacement with A displacement and tilt, might well operate differently at the two ends of the series, *i.e.* for zero tilts and large tilts. The role of directed bonds in compounds of Pb and Bi is obviously important, but not easily predicted. This approach too is indeterminate.

We conclude that the phenomenological correlation of strain with spontaneous polarization, translated into structural terms, is not a satisfactory explanation of these structures; and that the observed effects may be due to different factors in different materials.

7. Tilt angle and A-cation displacement in $R3c$ structures

In Fig. 6, the A-cation displacement parameters s listed in Table 7, are plotted against tilt angle ω.

Packing arguments suggest that, when the symmetry allows displacements of A cations along the triad axis, these will increase with decreasing size of A and hence with increasing tilt angle ω. The final column of Table 4 gives the dependence of the different A–O distances on s and ω. Neglecting ζ, which gives only a second-order effect, and terms in s^2, we find that the condition of equality of the six shortest distances is

$$s = \frac{\sin 2\omega}{24}(\sqrt{3} + \tan\omega) . \qquad (14)$$

The full line in Fig. 6 represents this condition.

The observed points show very considerable scatter about this line, indicating that equality of A–O distances is a relatively unimportant factor. It is of some interest that, while $NaNbO_3$, $LiNbO_3$, and $LiTaO_3$ all lie below the line, $BiFeO_3$ lies above it; there is still uncertainty about $PbZr_{0.90}Ti_{0.10}O_3$. Geometrically this means that in the first three structures the A cation is further from the face of the adjacent B octahedron than if all A–O bonds were equal, but in $BiFeO_3$ it is nearer. Movement *away* from a shared face between coordination polyhedra is expected in ionic structures as a consequence of cation–cation repulsion, and is commonly observed. Movement *towards* a shared face, like that in $BiFeO_3$, can only be explained in terms of directed bond formation.

Consideration of the relation between s and A-cation size would lead to the same conclusions; a graph of s *versus* $(r_A + r_O)/l$, with the equality condition

$$\left(\frac{r_A + r_O}{l}\right)^2 = 1 - 8s + 24s^2 \qquad (15)$$

would look very much like Fig. 6.

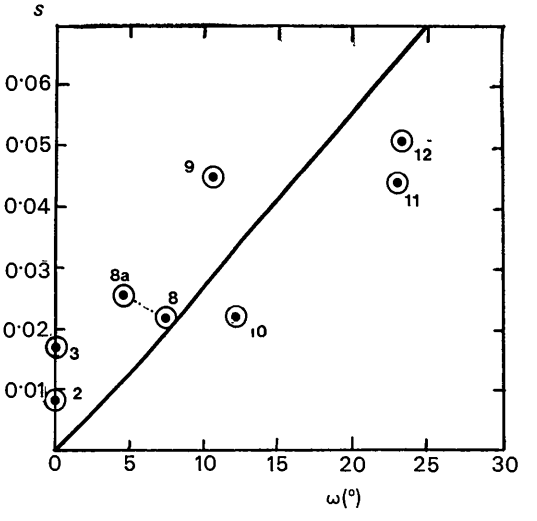

Fig. 6. A-cation parameter s *versus* tilt angle ω. Numbers of points refer to Table 7. The line is the condition for equality of six A–O distances, $s = (1/24)\sin 2\omega/(\sqrt{3} + \tan\omega)$.

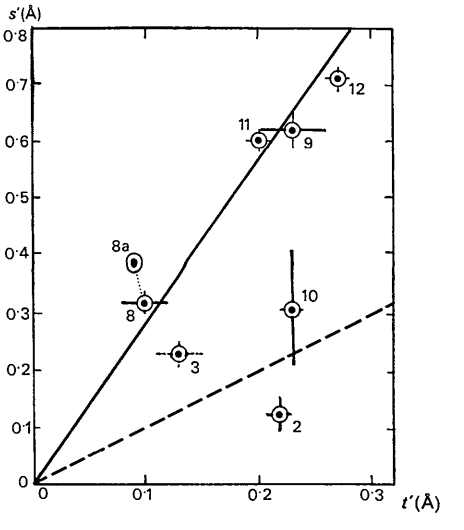

Fig. 7. A-cation displacement s' *versus* B-cation displacement t'. Experimental points numbered as in Table 7. Full line is that drawn by Michel *et al.* (1969*b*); dashed line is $s' = t'$.

8. A-cation displacement and B-cation displacement

The displacements, s' and t', are listed in Table 7, and are plotted against one another in Fig. 7.

Two straight lines are drawn on the figure. The full line represents an empirical relationship suggested by Michel, Moreau, Achenbach, Gerson & James (1969*b*). At the date of their paper, evidence for $NaNbO_3(N)$ and $KNbO_3$ was not available, and they ignored the *R*3*m* structure $PbZr_{0.58}Ti_{0.42}O_3$. Clearly the line can no longer be considered satisfactory. The dashed line represents the condition $s'=t'$, corresponding to an equally spaced array of cations.

These seems no theoretical reason to expect a simple universal relationship. There are at least three factors to be considered.

(i) For small high-valent B cations, displacement of B can be an intrinsic effect (Orgel, 1958; Megaw, 1968*a*). It is characteristic of a particular BO_6 octahedron in a particular temperature range, though subject to modification by temperature and by interaction with other factors. Here we are concerned only with intrinsic triad-axis displacement. Intrinsic triad-axis displacement is observed in $KNbO_3$ and $NaNbO_3(N)$, both low-temperature forms.

(ii) In the TaO_6 octahedron there is no intrinsic displacement, and at room temperature the NbO_6 octahedron shows intrinsic diad-axis displacement, not triad-axis. In both cases, however, the approach to the threshold for triad-axis displacement is sufficiently close to allow it to be surmounted by interaction with another factor – the tilt. In $LiTaO_3$ and $LiNbO_3$ the small Li cation is most stably accommodated in an octahedral environment, which can easily be achieved by a large triad-axis tilt combined with triad-axis displacement of Li. This decreases the shortest cation–cation distance, and the consequent A–B repulsion stabilizes and enhances the displacement of B.

Fig. 7 illustrates this effect for the niobates. Neglecting the temperature effect in $LiNbO_3$, we expect to find s' dependent, through the tilt, on A-cation size, and t' constant, to a first approximation. To a second approximation, t' should increase with A–B repulsion, and hence with s'. This is observed. The fact that $KNbO_3$ and $NaNbO_3(N)$ lie on different sides of the line $s'=t'$ is due to the different geometrical interaction of s' and tilt for different sizes of A. For $LiTaO_3$, where the intrinsic effect is further from the threshold than in $LiNbO_3$, both t' and s' are expected to be lower.

(iii) In compounds of Bi and Pb we may expect formation of directed bonds. By formation of strong trigonal bonds to three oxygen neighbours on one side, the A cation suffers displacement; at the same time, redistribution of the electron distribution round the oxygens changes their relation to B, and displacement of B follows.

The BO_6 groups found in these three compounds would not be expected to show intrinsic displacement of B. The (Zr,Ti) average atoms are larger than Ti, which itself is just below the threshold for intrinsic displacement. The difference of s' and t' in the two Pb compounds can be explained as follows, assuming that the bonding is the same in both. $Pb(Zr_{0.58}Ti_{0.42})O_3$ has the smaller B atom, and therefore, being nearer the intrinsic threshold, has the larger t'. On the other hand $Pb(Zr_{0.90}Ti_{0.10})O_3$ has the larger octahedron edge length l (*cf.* Table 5) and hence the smaller value of $(r_A+r_O)/l$, and the larger value of the tilt angle and of s'.

Though arguments from size are useful qualitatively, they cannot be pushed too far in making comparisons between structures where the character and degree of directed-bond formation differ.

9. Comparison with perovskites of other symmetries

The regularities and differences among the rhombohedral perovskites gain in interest when they are compared with effects in other perovskites. Only a very brief summary can be given here. (For a review of some of the structures, see Megaw, 1973.)

Geometrically, the simple orthorhombic perovskites fall into three groups. Corresponding to space group *R*3*m* we have *Bm*2*m*, represented by the orthorhombic forms of $BaTiO_3$ and $KNbO_3$. Corresponding to $R\bar{3}c$ we have *Pcmn* (or, in a different orientation, *Pbnm*) represented by the very numerous materials isomorphous with $CaTiO_3$ and $GdFeO_3$. Corresponding to *R*3*c* we have *P*2*mm*, the forced ferroelectric phase of $NaNbO_3$, *Q*. The first and third of these groups, as in their rhombohedral analogues, are characterized by B-cation displacement, the second and third by octahedron tilts, and there are interactions between displacements and tilts. The B displacements are however along the diad axis of the octahedron rather than the triad axis; there are two independent tilts about different axes; and A displacements are possible even when B displacements are forbidden. There are in addition more complex structures, *e.g.* $NaNbO_3(P)$, where additional factors or more complex interactions play a part. Examples of orthorhombic structures with directed bonds almost certainly occur, notably $PbZrO_3$, but the details are not well enough known to allow useful discussion.

Simple structures of tetragonal symmetry correspond to the first group (displacements only – *e.g.* tetragonal $BaTiO_3$ and $KNbO_3$) and the second group (tilts only – *e.g.* low-temperature $SrTiO_3$). Hitherto no simple tetragonal structures analogous to *R*3*c* have been found; combinations of tetrad-axis B displacements with tilts are more complex [*e.g.* $NaNbO_3(R)$]. The effect of directed-bond formation can however be seen in $PbTiO_3$.

One very interesting analogy concerns the octahedron strain. In orthorhombic perovskites this can have two independent components. In the series of rare-earth orthoferrites, both components can be seen to vary smoothly with A-cation radius and with the

components of tilt angle (Megaw, 1972, based on Marezio, Remeika & Dernier, 1970).

The occurrence of similar physical effects in structures of different symmetry helps to confirm their significance and also offers further opportunity to try and understand them.

10. Discussion

A study of correlations between parameters is aiming at something more than an empirical statement of systematic relationships. The correlations are a step towards recognizing structural factors of more general applicability. In the present work, we are clearly concerned with a number of such factors, varying in their relative importance in different materials. Where correlations exist, we are interested to distinguish which parameters are associated with the cause of the deformations, and which merely with the consequences.

Our discussion will be in terms of the 'static structure', *i.e.* of potential energy. Though a deeper treatment might need to introduce concepts of lattice dynamics, these themselves must be based (in so far as they are not simply phenomenological) on an understanding of the static structural forces. Thus the first analysis of a structure must be in terms of potential energy, not free energy.

The structural factors in terms of which the observed deformations are described are envisaged as independent, in the sense that they have their direct effects in different parts of the structure; but coupled, because no part of the structure is truly independent of the rest. Factors resulting in configurations known, from their widespread occurrence in a variety of structures, to be particularly stable may be regarded as the *cause* of a deformation; they give rise to a *local decrease* in potential energy. For example, the achievement of good packing, with interatomic distances nearly equal to the expected sum of the radii, is a common and important cause. More than one such cause may occur simultaneously. On the other hand, because of structural linkages, less stable groupings corresponding to *local increases* of potential energy may be imposed elsewhere; these, recognized by their unusual configurations, are *consequences* of the deformation. An illustration is given by the contrast between $LiNbO_3$ and $NaNbO_3$ (Megaw, 1974); in the former, the tilt is the cause (or stabiliser) of the triad-axis displacement, while in the latter the triad-axis displacement is the cause of the triad-axis tilt. The balance at which an overall minimum of potential energy is achieved depends on quantities analogous to elastic constants, relating the magnitude of each geometrical factor to the corresponding local stresses and local energy changes.

The causes of deformation with which we are here concerned include

(i) packing, *i.e.* the maintenance of contact between nearly rigid ions;
(ii) intrinsic off-centring of B cations;
(iii) directed-bond formation of certain cations (Pb and Bi);
(iv) a possible Jahn–Teller effect in $LaCoO_3$.

Coupling between these is in the first instance by the maintenance of the shared-corner linkage between octahedra, which translates the packing requirement into terms of tilt and (where symmetry allows) A displacement. Other coupling effects are cation–cation repulsion across the shared face of A and B polyhedra, and redistribution of the electron cloud round the oxygen atom. It is possible that the intrinsic non-spherical character of the oxygen atom should be regarded as a cause, associated with the departure from 180° of the B–O–B angle, but it is hard to formulate this quantitatively or to distinguish it from the simpler first-approximation packing effect.

11. Summary and conclusions

(i) It is useful to describe all rhombohedral perovskites in similar geometrical terms, which allow comparisons to be made and the real physical similarities and differences to be studied.

(ii) To a first approximation we can treat the BO_6 octahedra as regular. The observed rhombohedral interaxial angle (always a little less than 90°, or than 60°, according to the choice of axes of reference) is then a geometrical consequence of the tilt angle about the triad axis. The tilt angle depends primarily on packing round the A cation, and hence on the size of A, or more exactly, on the ratio $(r_A+r_O)/l$, where l is the octahedron edge length; small A cations give rise to large tilts.

(iii) At a second approximation, the strain (flattening or elongation) of the octahedron itself becomes significant. Systematic effects are found in compounds isomorphous with $LaAlO_3$, with space group $R\bar{3}c$ and fairly small tilt angles, where flattening of the octahedra increases with tilt angle. Qualitatively, the coupling is explained by systematic distortion of the non-spherical electron distribution round the oxygen atom.

(iv) Structures of space group $R3m$, and some of those of space group $R3c$, have elongated octahedra, but there is no simple correlation of strain with B-cation displacement.

(v) There is a general increase of A-cation displacement with tilt, and with decreasing A-cation size; this can be explained as a packing effect. The points show considerable scatter, which can partly be explained in terms of particular interatomic forces.

(vi) There is no simple universal relationship between A and B displacements, and no theoretical ground for expecting one. Comparisons of compounds with either A or B in common can be useful. Distinctions are drawn between those where the B displacement is either an intrinsic property of the octahedron or is easily induced by interaction with the tilt, and

those where the A displacement is primary, because of directed-bond formation by A.

(vii) Relationships observed in the rhombohedral perovskites bear a close analogy to those in perovskites of other symmetries, though the latter can show more complex combinations of effects.

References

ABRAHAMS, S. C. & BERNSTEIN, J. L. (1967). *J. Phys. Chem. Solids*, **28**, 1685–1692.

ABRAHAMS, S. C., HAMILTON, W. C. & REDDY, J. M. (1966). *J. Phys. Chem. Solids*, **27**, 1013–1018.

ABRAHAMS, S. C., HAMILTON, W. C. & SEQUEIRA, A. (1967). *J. Phys. Chem. Solids*, **28**, 1693–1698.

ABRAHAMS, S. C., KURTZ, S. K. & JAMIESON, P. B. (1968). *Phys. Rev.* **172**, 551–553.

ABRAHAMS, S. C., REDDY, J. M. & BERNSTEIN, J. L. (1966). *J. Phys. Chem. Solids*, **27**, 997–1012.

BURBANK, R. D. (1970). *J. Appl. Cryst.* **3**, 112–120.

DALZIEL, J. A. W. & WELCH, A. J. E. (1960). *Acta Cryst.* **13**, 956–958.

DARLINGTON, C. N. W. & MEGAW, H. D. (1973). *Acta Cryst.* B**29**, 2171–2185.

GELLER, S. (1957). *Acta Cryst.* **10**, 243–251.

GELLER, S. & BALA, V. B. (1956). *Acta Cryst.* **9**, 1019–1025.

HARLEY, R. J., HAYES, W., PERRY, A. M. & SMITH, S. R. P. (1973). *J. Phys. C: Solid State Phys.* **6**, 2382–2400.

HEPWORTH, M. A., JACK, K. H., PEACOCK, R. D. & WESTLAND, G. J. (1957). *Acta Cryst.* **10**, 63–69.

HEWAT, A. W. (1973). *J. Phys. C: Solid State Phys.* **6**, 2559–2572.

JACOBSON, A. J., TOFIELD, B. C. & FENDER, B. E. F. (1972). *Acta Cryst.* B**28**, 956–961.

KAY, H. F. & VOUSDEN, P. (1949). *Phil. Mag. Ser.* 7, **40**, 1019–1040.

KIM, Y. S. (1968). *Acta Cryst.* B**24**, 295–296.

MAREZIO, M., REMEIKA, J. P. & DERNIER, P. D. (1970). *Acta Cryst.* B**26**, 2008–2022.

MEGAW, H. D. (1968*a*). *Acta Cryst.* B**24**, 149–153.

MEGAW, H. D. (1968*b*). *Acta Cryst.* A**24**, 583–588.

MEGAW, H. D. (1968*c*). *Acta Cryst.* A**24**, 589–604.

MEGAW, H. D. (1972). *J. Physique*, **33**, *Suppl.* C2, 1–5.

MEGAW, H. D. (1973). *Crystal Structures: A Working Approach.* Philadelphia: Saunders.

MEGAW, H. D. (1974). *Ferroelectrics*, **7**, 87–89.

MENYUK, N., DWIGHT, K. & RACCAH, P. M. (1967). *J. Phys. Chem. Solids*, **28**, 549–556.

MICHEL, C., MOREAU, J. M., ACHENBACH, G. D., GERSON, R. & JAMES, W. J. (1969*a*). *Solid State Commun.* **7**, 701–704.

MICHEL, C., MOREAU, J. M., ACHENBACH, G. D., GERSON, R. & JAMES, W. J. (1969*b*). *Solid State Commun.* **7**, 865–868.

MICHEL, C., MOREAU, J. M. & JAMES, W. J. (1971). *Acta Cryst.* B**27**, 501–503.

MICHEL, C., MOREAU, J. M. & JAMES, W. J. (1972). *Acta Cryst.* B**28**, 3674.

MOREAU, J. M., MICHEL, C., GERSON, R. & JAMES, W. J. (1970). *Acta Cryst.* B**26**, 1425–1428.

MÜLLER, K. A., BERLINGER, W. & WALDNER, F. (1968). *Phys. Rev. Lett.* **21**, 814–817.

ORGEL, L. E. (1958). *Faraday Soc. Discuss.* **26**, 138–144.

SHANNON, R. D. & PREWITT, C. T. (1969). *Acta Cryst.* B**25**, 925-946.

SHANNON, R. D. & PREWITT, C. T. (1970). *Acta Cryst.* B**26**, 1046–1048.

TOMAŠPOL'SKIJ, JU. JA., VENEVCEV, JU. N. & ŽDANOV, G. S. (1964). *Kristallografija*, **9**, 846–852; *Sov. Phys. Crystallogr.* **9**, 715–720.

VENEVCEV, JU. N., ŽDANOV, G. S., SOLOV'EV, S. P., BEZUS, E. V., IVANOVA, V. V., FEDULOV, S. A. & KAPYŠEV, A. G. (1960). *Kristallografija*, **5**, 620–626. *Sov. Phys. Crystallogr.* **5**, 594–599.

WOLD, A., POST, B. & BANKS, E. (1957). *J. Amer. Chem. Soc.* **79**, 6365–6366.